Nonlinear loss dynamics in a silicon slow-light photonic crystal waveguide

Bill Corcoran,[1,*] Christelle Monat,[1] Dominik Pudo,[1] Benjamin J. Eggleton,[1] Thomas F. Krauss,[2] David J. Moss,[1] Liam O'Faolain,[2] Mark Pelusi,[1] and Thomas P. White[2]

[1]*Centre for Ultrahigh-Bandwidth Devices for Optical Systems (CUDOS), Institute for Photonics and Optical Sciences (IPOS), School of Physics, University of Sydney, New South Wales 2006, Australia*

[2]*School of Physics and Astronomy, University of St Andrews, St Andrews, Fife KY16 9SS, United Kingdom*

**Corresponding author: billc@physics.usyd.edu.au*

Received December 10, 2009; revised February 10, 2010; accepted February 14, 2010; posted March 2, 2010 (Doc. ID 121203); published March 31, 2010

We directly investigate both experimentally and numerically the influence of optical nonlinear loss dynamics on a silicon waveguide based all-optical device. The dynamics of these nonlinear losses are explored through the analysis of optical limiting of an amplitude distorted 10 Gbit/s signal in a slow-light silicon photonic crystal waveguide. As the frequency of the distortion approaches the free-carrier recombination rate, free-carrier absorption reaches a steady state, leaving two-photon absorption the dominant dynamic nonlinear loss. Our results highlight the importance of engineering the free-carrier lifetime in silicon waveguides for high speed all-optical processing applications. © 2010 Optical Society of America

OCIS codes: 190.4390, 130.5296.

As communication systems approach the speed limits of electronics, all-optical processes present a way to push signal manipulation past the boundary of gigahertz processes and into the terahertz regime. Silicon, the material of choice for the microelectronics industry, is gaining ground as a platform for all-optical devices [1–3]. In this semiconductor material, all-optical processes utilizing intensity dependent optical nonlinearities are generally accompanied by a significant level of nonlinear loss, which in many cases has a detrimental impact on the device operation [4,5], but can be useful for some functions such as optical limiting. As such, the operation of fast all-optical devices on silicon will be affected by the dynamics of nonlinear losses.

Nonlinear loss in silicon is comprised of two mechanisms: the quasi-instantaneous effect of two-photon absorption (TPA) and the longer lived effect of absorption by free carriers [free-carrier absorption (FCA)]—generated in silicon through TPA [6,7]. The magnitude of FCA is determined by the amount of free carriers in the waveguide, so the dynamics of free carriers as dictated by their lifetime τ_c is expected to impact upon optical limiting. Planar photonic crystal (PhC) waveguides provide a unique platform for enhancing waveguide nonlinearity through both tight modal confinement and slow light [7–11]. This has been demonstrated to increase the efficiency per unit length of nonlinear processes [12–16], including nonlinear loss [12–14]. Recently we demonstrated the regeneration of a 10 Gbit/s signal through a short (80 μm) dispersion engineered slow-light silicon PhC waveguide that acts as an efficient optical limiter through nonlinear loss (concept represented in Fig. 1) [17]. The influence of nonlinear loss dynamics, however, was left as an open question in [17] and is a key to understanding the impact of free-carrier lifetime on all-optical processes in silicon.

In this work, we directly investigate the effect of free-carrier dynamics on optical limiting of a 10 Gbit/s data stream in an 80-μm-long dispersion engineered silicon PhC waveguide by varying the speed of the amplitude fluctuation imposed on the optical data. We show that the dynamics of free carriers allow FCA to complement TPA in compensating for amplitude distortions below the gigahertz regime, but degrade optical limiting for high distortion frequencies, highlighting the need for control of the free-carrier lifetime for high-speed all-optical devices in silicon.

The experimental setup (Fig. 1), used to investigate the effect of free-carrier dynamics on optical limiting, is similar to [17]. The signal consists of a 10 Gbit/s data stream [return-to-zero, 2% duty cycle, 2^{31}-1 pattern length pseudo-random bit sequence (PRBS)], the "1" level of which is distorted by applying an asynchronous radio-frequency modulation at a frequency f_d varied between 10 MHZ and 5 GHz. This signal is coupled to a modified $W1$ waveguide (lattice period of $a=410$ nm, hole radius of $r=0.286a$) with a

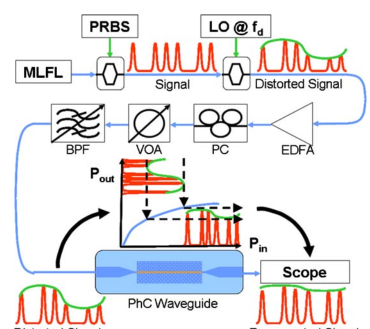

Fig. 1. (Color online) Optical limiting schematic. A nonlinear power transfer function with transmission decreasing for high input powers (in this case provided by nonlinear loss in the PhC waveguide) allows for the reduction in amplitude fluctuation. Pulses from a 10 GHz mode-locked fiber laser (MLFL) are imprinted with a 10 Gbit/s PRBS, amplitude distorted at a frequency f_d by a local oscillator (LO), amplified (30 dBm maximum erbium-doped fiber amplifier), passed through a polarization controller (PC), variable optical attenuator (VOA), and a 5 nm bandpass filter (BPF), then butt-coupled to the PhC waveguide chip.

low group velocity ($c/40$) and reduced dispersion, providing an increased amount of nonlinear loss per unit length [11,12,16]. The statistical distribution of the "1" level of the eye diagram at the output of the waveguide [Figs. 2(a) and 2(b), measured by an Agilent Infinium DCA, 65 GHz photodetector bandwidth] gives a measure of the signal amplitude distortion for each f_d. By comparing results for the operation in both low-power (linear, 20 mW coupled peak power) and high-power (nonlinear, 1 W coupled peak power) regimes, we infer a relative figure of the distortion reduction (DR) afforded by the power limiting action of the device.

Practically, we define the distortion Δ of the "1" level of the optical data as the ratio of the standard deviation to the mean ($\sigma/\langle P\rangle$) of the "1" level. The standard deviation we use (σ) has dark noise (σ_{dark} measured with no input to the oscilloscope) subtracted from the measured deviation of the "1" level [σ_1 as per Fig. 2(a)], i.e., $\sigma=(\sigma_1{}^2-\sigma_{\text{dark}}{}^2)^{0.5}$. Note that although a relative decrease in Δ will indicate a relative increase in the quality factor of the eye $Q=(\langle P_1\rangle-\langle P_0\rangle)/(\sigma_1+\sigma_0)$, the changes in Δ due to optical limiting will be more dramatic than changes in Q since the device action only improves the "1" level statistic distribution—and not the "0" level. While the metric Δ does not measure system improvement (i.e., bit-error rate), it directly reflects the effect of optical limiting functionality of our device. We define the DR afforded by the waveguide on the "1" level as the ratio of the associated signal distortion measured at low and high powers, i.e., $\text{DR}=(1-\Delta_{\text{high}}/\Delta_{\text{low}})\times 100$. Measurements [Fig. 2(c)] show that the DR drops as the frequency of applied distortion f_d increases and exhibits three distinct regimes. For f_d below 50 MHz [region (a)], we achieve a maximum level of DR of ~35% (i.e., fluctuation of the "1" level is reduced by ~35%), near invariant with f_d. Between 50 and 500 MHz [region (b)], the DR rolls off with increasing f_d. Above 500 MHz, the DR reaches a lower bound (of ~15%) and changes little with further increasing f_d [region (c)].

In order to understand this behavior, the PhC waveguide is modeled using the nonlinear Schrodinger equation given by Eq. (1) [12],

$$\frac{\partial A}{dz}+\frac{i\beta_2}{2}\frac{\partial^2 A}{dz^2}+S\frac{\alpha}{2}A=iS^2\gamma(|A^2|A)-S^2\frac{\beta_{\text{TPA}}}{2A_{\text{eff}}}+SN_C\frac{2\pi i k_C}{\lambda_0}A-SN_C\frac{\sigma}{2}A. \quad (1)$$

This model approximates the propagation of optical pulses with a slowly varying electric field envelope A in the three-dimensional PhC waveguide structure to a one-dimensional problem and accounts for the slow-light enhancement of the various terms by including the slow-down factor $S=v_{g(\text{fast})}/v_{g(\text{slow})}$. This equation is coupled with a rate equation for photogeneration of free carriers through TPA [6] to calculate the free-carrier density N_c in the waveguide. Material parameters (k_C, σ, β_{TPA}, and n_2) are as in [6,12], while the PhC waveguide parameters, i.e., the second-order dispersion coefficient β_2, the effective area A_{eff}, the linear loss α, and the slow-down factor S are, respectively, equal to 1×10^{-21} s^2/m, 0.57 μm^2, 20 dB/cm, and 11. Equation (1) is evaluated numerically using the split-step Fourier method (SSFM), for a train of 2 ps pulses at a 10 GHz repetition rate, with amplitude sinusoidally varying at a frequency f_d. The comparison of the peak to peak amplitude of the envelope of the modulated pulse train at output and input provides an analogous measure to the DR of the "1" level studied experimentally. The simulated frequency dependence of the DR using this model is shown in Fig. 2(c) (red squares) for a free-carrier lifetime τ_c of 1 ns and matches well with the measured DR.

We numerically investigate the separate contributions of the FCA and TPA to optical limiting. Without the FCA, instantaneous TPA provides a DR that is invariant with the applied distortion frequency as expected [blue triangles in Fig. 3(a)], so the changing behavior between regions (a) and (b) in Fig. 2(c) must be a consequence of the dynamics of FCA. By artificially decoupling FCA and TPA through removing the TPA loss term in Eq. (1), we find that the DR due to FCA continuously decreases [green dots in Fig. 3(a)], with increasing distortion frequency, and becomes negligible for $f_d>1$ GHz. By varying τ_c between 0.2 and 1 ns in the simulations (including both TPA and FCA), Fig. 3(b) shows that short recombination times allow the FCA to be an effective optical limiting mechanism for faster optical distortions. The DR roll-

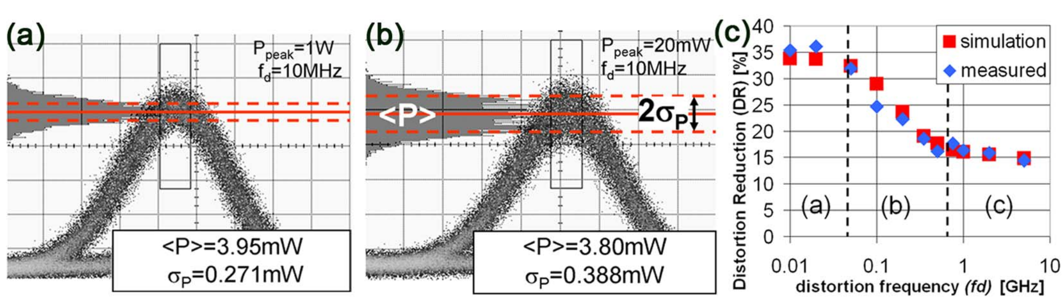

Fig. 2. (Color online) (a) Sample eye diagram for high input power. Box indicates sampled "1" level, distortion measured from σ_1 and $\langle P\rangle$. (b) Corresponding low input power eye diagram to (a). (c) Change in DR in the "1" level data when varying the frequency of the superimposed distortion; simulated values are from the SSFM model (with both TPA and FCA, $\tau_c=1$ ns).

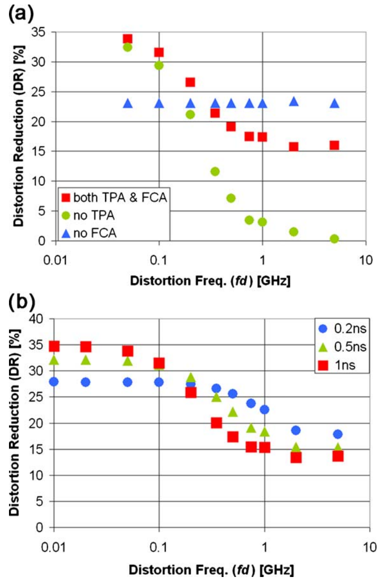

Fig. 3. (Color online) Simulated DR using SSFM. For comparison: red square traces here are the same as the simulated trace in Fig. 2. (a) Different traces simulated by removing terms from Eq. (1), as indicated in the legend. (b) Different traces simulated with both TPA and FCA for different values of τ_c between 0.2 and 1 ns.

off frequency increases from ~50 MHz for $\tau_c = 1$ ns to ~200 MHz for $\tau_c = 0.2$ ns, i.e., close to $0.05/\tau_c$. The free-carrier density must change at the same speed as the distortion for FCA to suppress amplitude fluctuations; otherwise FCA will form a steady-state loss. Therefore, FCA only plays an effective role in optical limiting as long as their recombination is significantly faster (here by 1 order of magnitude) than the amplitude fluctuations. In section (a) [Fig. 2(c)], the distortion frequency is slow enough that FCA can contribute to optical limiting. The DR reduces in region (b) along with the FCA contribution. In region (c), the DR reaches a lower bound where instantaneous TPA alone affords some DR, which is less than what is expected from TPA alone [blue triangles in Fig. 3(a)] due to the steady-state FCA loss at high f_d.

The free-carrier lifetime in PhC waveguides varies significantly—between 400 ps and 2 ns [18,19]—due to factors like waveguide processing and geometry. In this work, we infer the free-carrier lifetime (τ_c) by fitting theory to experiment. The inferred value of $\tau_c = 1$ ns lies within the expected range. Various schemes can reduce τ_c in waveguides [4,20], which should let FCA remain a dynamic nonlinear loss for faster optical intensity variations, in this case allowing for optical limiting of faster amplitude fluctuations. Note however that, as illustrated in Fig. 3(b), a lower τ_c reduces the maximum DR afforded by the device due to the associated decrease in the average FCA; this suggests that for optical limiting applications, there is a trade-off value for τ_c.

In conclusion, we have experimentally and numerically investigated the effect of nonlinear loss dynamics on optical limiting in a short slow-light PhC waveguide. We find that for slowly varying optical intensity fluctuations (at frequencies below $\sim 0.05/\tau_c$), slow-light enhanced nonlinear loss due to free carriers works together with TPA. However, as fluctuation speeds approach the free-carrier lifetime in the waveguide, the free-carrier contribution to optical limiting strongly decreases until vanishing completely (at a frequency on order of $1/\tau_c$). Modeling allows us to describe the transition of the FCA from a dynamic to steady-state loss, which restricts high speed performance of all-optical devices like optical limiters unless steps are taken in the fabrication to accelerate free-carrier recombination.

The support of the Australian Research Council through its Centre of Excellence and Discovery Grant programs is gratefully acknowledged. Additional acknowledgement is given to the support of the Department of Education, Science and Technology through the International Science Linkages program. The silicon samples were fabricated in the framework of the EU-FP6-funded ePIXnet Nanostructuring Platform for Photonic Integration.

References

1. M. Lipson, Electron. Lett. **45**, 576 (2009).
2. B. Jalali, Phys. Status Solidi A **205**, 213 (2008).
3. Q. Lin, O. Painter, and G. P. Agrawal, Opt. Express **15**, 16604 (2007).
4. H. Rong, A. Liu, R. Jones, O. Cohen, D. Hak, R. Nicolaescu, A. Fang, and M. Paniccia, Nature **433**, 292 (2005).
5. M. Foster, A. Turner, R. Salem, M. Lipson, and A. Gaeta, Opt. Express **15**, 12949 (2007).
6. L. Yin and G. P. Agrawal, Opt. Lett. **32**, 2031 (2007).
7. R. Soref, IEEE J. Sel. Top. Quantum Electron. **22**, 873 (1986).
8. T. F. Krauss, J. Phys. D **40**, 2666 (2007).
9. M. Soljacic and J. D. Joannopoulos, Nature Mater. **3**, 211 (2004).
10. M. D. Settle, R. J. P. Engelen, M. Salib, A. Michaeli, L. Kuipers, and T. F. Krauss, Opt. Express **15**, 219 (2007).
11. C. Monat, B. Corcoran, D. Pudo, M. Ebnaili-Heidari, C. Grillet, M. D. Pelusi, D. J. Moss, B. J. Eggleton, T. P. White, L. O'Faolain, and T. F. Krauss, IEEE J. Sel. Top. Quantum Electron. **16**, 334 (2010).
12. C. Monat, B. Corcoran, M. Ebnaili-Heidari, C. Grillet, B. J. Eggleton, T. P. White, L. O'Faolain, and T. F. Krauss, Opt. Express **17**, 2944 (2009).
13. A. Baron, A. Ryasnyanskiuy, N. Dubreuil, P. Delaye, Q. V. Tran, S. Combrie, A. de Rossi, R. Frey, and G. Roosen, Opt. Express **17**, 552 (2009).
14. H. Hamachi, S. Kubo, and T. Baba, Opt. Lett. **34**, 1072 (2009).
15. K. Inoue, H. Oda, N. Ikeda, and K. Asakawa, Opt. Express **17**, 7206 (2009).
16. B. Corcoran, C. Monat, C. Grillet, D. J. Moss, B. J. Eggleton, T. P. White, L. O'Faolain, and T. K. Krauss, Nat. Photonics **3**, 206 (2009).
17. D. Pudo, B. Corcoran, C. Monat, M. Pelusi, D. Moss, B. J. Eggleton, T. P. White, L. O'Faolain, and T. F. Krauss, Photonics Nanostruct. Fundam. Appl., doi:10.1016/j.photonics.2009.08.002.
18. T. Kampfrath, D. Beggs, T. P. White, M. Burresi, D. van Oosten, T. F. Krauss, and L. Kuipers, Appl. Phys. Lett. **94**, 241119 (2009).
19. F. Ndi, J. Toulouse, T. Hodson, and D. W. Prather, Opt. Lett. **30**, 2254 (2005).
20. F. Doany, D. Grischkowsky, and C. C. Chi, Appl. Phys. Lett. **50**, 460 (1987).